Storm surge hydrographs and characteristics along the Dutch coast. An analysis from simulation data

Caspers, Jochem J.; Kindermann, Paulina E.; Rongen, Guus W.F.; Geerse, Chris P.M.

DOI
10.1016/j.coastaleng.2025.104776

Publication date
2025

Document Version
Final published version

Published in
Coastal Engineering

Citation (APA)
Caspers, J. J., Kindermann, P. E., Rongen, G. W. F., & Geerse, C. P. M. (2025). Storm surge hydrographs and characteristics along the Dutch coast. An analysis from simulation data. *Coastal Engineering*, *201*, Article 104776. https://doi.org/10.1016/j.coastaleng.2025.104776

Coastal Engineering 201 (2025) 104776

Contents lists available at ScienceDirect

Coastal Engineering

journal homepage: www.elsevier.com/locate/coastaleng

Storm surge hydrographs and characteristics along the Dutch coast. An analysis from simulation data

Jochem J. Caspers [a,1], Paulina E. Kindermann [a,b,*,1], Guus W.F. Rongen [a,b], Chris P.M. Geerse [a]

[a] HKV Lijn in Water, Botter 11-29, Lelystad, 8232 JN, The Netherlands
[b] Department of Hydraulic Engineering, Faculty of Civil Engineering and Geosciences, Delft University of Technology, Stevinweg 1, Delft, 2628 CN, The Netherlands

ARTICLE INFO

Keywords:
Storm surge hydrographs
Extreme sea levels
Reanalysis data
Storm characterization
Flood risk assessments

ABSTRACT

This study analyzes storm characteristics and surge hydrographs corresponding to extreme storms in the Dutch coastal area, using a large dataset from simulated time series. A total of 8,000 storm events were selected for four study locations, allowing for a comprehensive investigation of various storm characteristics. Findings reveal that the offset between maximum surge and astronomical high tide typically exhibits three predominant values. A new percentile method for averaging storm surge hydrographs was employed, effectively preserving a realistic shape of the storm surge hydrograph and accurately reflecting durations. Comparing the averaged storm surge hydrographs for different magnitudes of the surge peak shows that it is possible to scale the averaged storm surge hydrograph to any peak value, as long as storms are first clustered based on location, tidal offset, and exceedance duration, since these characteristics substantially impact the shape of storm surge hydrographs. Comparisons with current design guidelines show that prescribed storm surge hydrographs often underestimate durations on the flanks of storm events, with variations in peak characteristics depending on location. The insights gained in this study, can be used to improve the representation of hydraulic loads in flood defense guidelines, potentially leading to more accurate flood safety assessments for coastal infrastructure.

1. Introduction

The Dutch coast protects a low-lying, densely populated hinterland that is prone to flooding from the sea. Extreme sea levels along the Dutch coast are caused by storm surges in the North Sea, driven by high wind speeds. Therefore, flood defenses along the Dutch coast are designed to sustain extreme sea levels and wave heights with return periods of 1,000 years or more, according to Dutch safety standards (Jonkman and Schweckendiek, 2015; Jongejan et al., 2016). The derivation of these design conditions relies heavily on statistical extrapolation, since observations are only available for the past 100 to 150 years. Consequently, the return periods of specific extreme wind speeds and sea levels are uncertain. Moreover, the current guidelines for (semi-)probabilistic reliability assessments of coastal flood defenses, called WBI (in Dutch: Wettelijk Beoordelingsinstrumentarium), only prescribe the maximum wind speed, maximum sea level and the wind direction during maximum wind speed as stochastic variables (Chbab and de Waal, 2017). Other storm characteristics, such as the duration of the storm or the time offset between high tide and maximum surge, are included as fixed values. As a consequence, the current approach relies on one sea level hydrograph, which is schematized by the sum of the astronomical tide and the residual surge. The corresponding surge hydrograph has a trapezoidal shape with a fixed duration and timing with respect to high tide. This schematization was derived from horizontally averaging over a set of normalized storm surge hydrographs from observational data (Chbab, 2015b). The above-mentioned simplifications are motivated by both the limited knowledge of these variables under extreme conditions from observations and the need to reduce model complexity.

In reality, however, storm duration and tidal offset can vary significantly between extreme storms, as illustrated in Fig. 1. The figure presents the observed sea level and surge hydrographs for two historical, extreme events at Hoek van Holland. Alongside, the schematized surge hydrograph is plotted according to current guidelines. The figure reveals that the devastating storm event of January, 1953, exhibited a relatively long duration of the storm surge, exceeding a level of NAP+2 m for about 3 h longer than the schematized surge hydrograph from WBI. In contrast, storm Pia, which triggered the unprecedented closure of the Maeslant storm surge barrier in December 2023, was

* Corresponding author at: Department of Hydraulic Engineering, Faculty of Civil Engineering and Geosciences, Delft University of Technology, Stevinweg 1, Delft, 2628 CN, The Netherlands.
E-mail address: p.e.kindermann@tudelft.nl (P.E. Kindermann).
[1] Joint first authorship.

https://doi.org/10.1016/j.coastaleng.2025.104776
Received 17 December 2024; Received in revised form 7 May 2025; Accepted 8 May 2025
Available online 26 May 2025

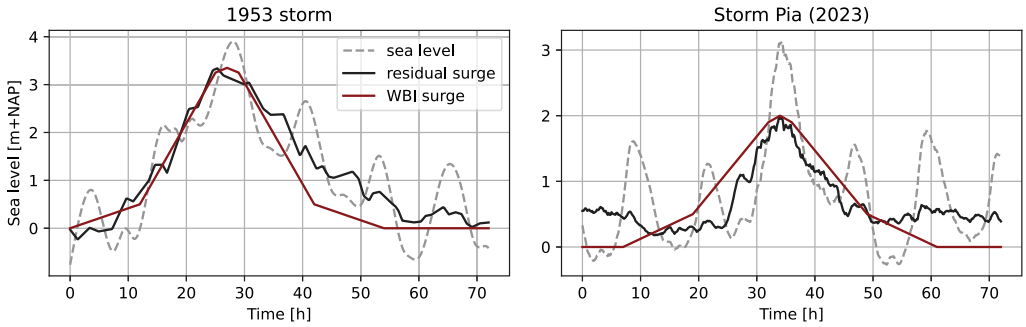

Fig. 1. Hydrographs of sea level (dashed gray) and residual surge (black) for two observed storm events at Hoek van Holland: the 1953-storm (left) and storm Pia in December, 2023 (right). The schematized hydrograph from the current Dutch design guidelines (WBI) is plotted in red. The observation data is retrieved from Deltacommissie (1961) for the 1953-storm and from waterinfo.rws.nl by Rijkswaterstaat (2024) for Pia.

relatively short compared to the WBI surge hydrograph. Besides, both observed storms revealed a small time offset between maximum storm surge and high tide: about 2 h for the 1953-storm and 1.5 h for storm Pia, while the current guidelines prescribe a fixed value of −4.5 h for the tidal offset (note that this is not illustrated in Fig. 1).

Most failure mechanisms of coastal flood defenses are time-dependent erosion processes, for which the duration of the event, the timing with respect to tide and the rotation of the wind play an important role. By relying on only two stochastic variables (wind speed and sea level) and a single hydrograph shape, current assessments may not fully capture the variability of extreme events, which could lead to less representative reliability estimates for flood defenses.

There are several ways to overcome the underlying problem of data scarcity and include more random variables in extreme sea level schematizations. One option is to make use of stochastic models, which is already commonly used in flood risk assessments in the Netherlands and abroad. For instance, in the study by MacPherson et al. (2019), a stochastic model for the German Baltic Sea coast was developed, which is capable of simulating the temporal behavior of extreme sea levels. The model input was defined by parameterizing hydrographs of extreme sea levels from 45 tide-gauges and fitting parametric distribution functions to the observed parameter data. Diakomopoulos et al. (2024) statistically investigated driving mechanisms to improve estimations of extreme sea levels for flood risk assessments. While these are good examples of applicable, probabilistic frameworks for flood risk assessments, both studies are based on a limited number of observed extreme events, introducing substantial uncertainty in the fitted distribution when extrapolating towards return periods of a 1,000 years or more.

Another option is using data from numerical models. In recent years, run times of meteorological and hydrological models have decreased, which has increased the availability of large datasets of simulated wind and sea level data (Hersbach et al., 2017; National Center for Atmospheric Research Staff (Eds), 2022). These datasets have a great potential to improve our understanding of extreme storms, and their natural variability in both space and time (Muis et al., 2023; Dullaart et al., 2023). For example, Dullaart et al. (2023) have developed a method to generate a global dataset of hydrographs, based on time series of storm surges and tides derived from the Global Tide and Surge Model (GTSM) forced with the ERA5 reanalysis wind and pressure fields, for the period from 1980 to 2017.

Still, the limitation of most studies that use numerical model results, is the relatively short datasets (up to 66 years in MacPherson et al. (2019) and 38 years for Dullaart et al. (2023)), which is rather short to extrapolate to return periods of up to 10,000 years, that are relevant in the Dutch flood safety approach. For this reason, the Royal Dutch Meteorological Institute (KNMI) has produced a very large dataset of simulated sea levels, using the WAQUA-DCSMv5 model forced with wind fields from the seasonal forecasting system (SEAS5) by the European Centre for Medium-Range Weather Forecasts (ECMWF, 2021). By considering each ensemble member from SEAS5 as being a possible realization of weather under current climate conditions, a synthetic time series of approximately 8,000 years was created. This extensive dataset can be used to derive higher-precision estimates for the return levels of extreme wind speeds and sea levels, which is currently being investigated by the KNMI on behalf of Rijkswaterstaat, which is the Department of Waterways and Public Works of the Dutch Ministry of Infrastructure and Water Management (de Valk and van den Brink, 2023, 2025). Additionally, these long time series give the opportunity to improve our understanding of the physical, spatial and temporal behavior of extreme storms.

In this study, we examine how various storm characteristics influence the shape of surge hydrographs along the Dutch coast. We extract time series of sea level, residual surge and (predicted) astronomical tide for extreme storm events from the KNMI-dataset, then cluster storm events based on relevant storm surge characteristics, and analyze the surge hydrographs for each cluster. Based on this, we propose a set of representative surge hydrographs that can be used for design and assessment of coastal flood defenses in the Netherlands. In doing so, we contribute to the development of a new stochastic model for describing the hydraulic loads at the Dutch coast, which is currently being researched by Rijkswaterstaat.

2. Data and study area

We have used the dataset that was produced by KNMI (van den Brink, 2020), consisting of simulated sea levels from the WAQUA-DCSMv5 model, which was forced with wind fields from the seasonal forecasting system (SEAS5) by ECMWF (ECMWF, 2021). Since November 2017, ECMWF's seasonal forecasts are initiated on the first of every month and run for the upcoming seven months, consisting of 51 ensemble members. For 1981–2016, hindcasts were produced for system calibration, consisting of 51 ensemble members for the start dates on the first of February, May, August and November, and 25 members for the other months. In a statistical sense, each ensemble member can be considered as a possible realization of meteorological conditions in the current climate, which enables merging them into one large dataset equivalent of approximately 8,000 years of data. van den Brink (2020) have excluded the first month of each ensemble member, to avoid mutual dependence between ensemble members. From each ensemble, KNMI has used the 6-hourly mean sea level pressure and surface stress fields as input to run the WAQUA-DCSMv5 model, and the astronomical tide at the open boundaries was derived by harmonic expansion using ten tidal constituents. The model output consists of sea levels and astronomical tide in the North Sea with a 10 min resolution, corresponding to the wind fields from each SEAS5 ensemble member. The input and output of WAQUA-DCSMv5 cover a domain of the northwest European continental shelf, more specifically between 15° W to 13° E and 43° N to 64° N (Gerritsen et al., 1995). The so-called Dutch Continental Shelf Model (DCSM) is a numerical model that

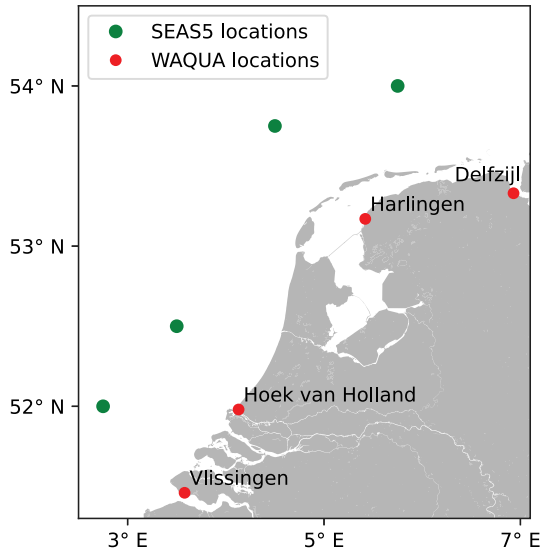

Fig. 2. Map with the selected locations for which we extract the sea level time series from the SEAS5/WAQUA-DCSMv5 dataset indicated in red and the locations where we determine the corresponding wind data from the SEAS5 grid in green.

solves the two-dimensional shallow-water equations on a $\frac{1}{8}^{\circ} \times \frac{1}{12}^{\circ}$ grid. DCSM was originally developed in the 1980s and has been through numerous improvements since then (Verlaan et al., 2005). In 2022, the sixth-generation of the model (3D DCSM-FM) was released, while in operational forecasting for the Dutch coast the fifth version (DCSMv6) is currently used (Zijl et al., 2022). Since these new versions of the model are computationally more extensive, KNMI has used the fourth-generation of the model (WAQUA-DCSMv5) to simulate the sea levels on the North Sea corresponding to the SEAS5 ensemble members. A comparison was made with newer model versions and observations, which resulted in a bias correction of 10%. Additionally, resulting wind statistics were compared to observations and to results from the regional climate model RACMO. Consequently, van den Brink (2020), de Valk and van den Brink (2025) concluded that the resulting model data are sufficiently close to the observed data to consider them samples from the same population. Therefore, the resulting output of wind and sea levels can be considered a 8,000-year synthetic dataset of the current climate, and statistical properties can be extracted accordingly. For more details about the creation and validation of this dataset we refer to de Valk and van den Brink (2025), van den Brink (2020).

2.1. Study area

We focused on four locations along the Dutch North Sea coast, as shown in Fig. 2. For these four locations, we have extracted the nearest sea level grid point data from the WAQUA-DCSMv5 model output (indicated by red points in Fig. 2). The wind direction and wind speed data for each location were extracted from one nearby SEAS5 grid cells. These SEAS5 grid cells were chosen with considerable distance from the coast to ensure that no influence of the land on the surface roughness can be expected. Since extreme surges at the Dutch coast typically occur for large depressions with strong wind speeds over large parts of the North sea, grid points further from the coast appear to be an appropriate choice (van den Brink, 2020). KNMI has used the same sea level grid points to derive estimates for return levels of extreme wind speeds and sea levels for the Dutch design guidelines (de Valk and van den Brink, 2023, 2025).

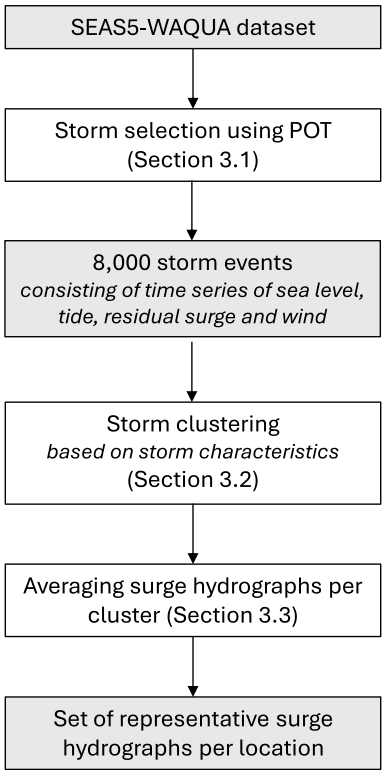

Fig. 3. Schematized illustration of the methodology for one location, with datasets indicated in gray and steps of the method in white.

Table 1
Thresholds (in m+NAP) for the peaks-over-thresholds that result in the selection of 8000 storm events.

Vlissingen	Hoek van Holland	Harlingen	Delfzijl
3.51	2.29	2.55	3.12

3. Methodology

Fig. 3 provides an overview of the method. First, storms were selected from the selected grid points from the SEAS5-WAQUA dataset by KNMI, using peaks-over-thresholds (POT). This is described in Section 3.1. Next, storms were clustered based on specific storm characteristics, with both the clustering process and methodology detailed in Section 3.2. Finally, representative surge hydrographs for each cluster were obtained by averaging the surge hydrographs of individual storms within the cluster, as explained in Section 3.3.

3.1. Storm selection

Extreme storm events were selected from the SEAS5-DCSMv5 time series corresponding to the grid points shown in Fig. 2, using the POT-method based on sea level. For each coastal location, the POT-threshold was chosen such that the 8,000 highest sea level events were selected, corresponding to on average one storm event per year. The resulting thresholds are presented in Table 1. As a reference, the storm selection for Vlissingen contains 56 storm events with sea levels exceeding those of the 1953-storm, which resulted in the highest sea level ever recorded at the Dutch coast.

To ensure independence of selected storm events, a rolling window of three days was applied. From an analysis of observational data by Tijssen and Diermanse (2010), it was concluded that both wind and storm surge durations at Hoek van Holland are on average 48 h, varying between 37 and 78 h, depending on the chosen time window, threshold

value and approach for secondary peak. Therefore we presume that a three-day window is a safe and appropriate choice to distinguish individual storm events and to ensure that surge hydrographs are not strongly influenced by preceding storm events.

Subsequently, time series of wind speed, wind direction, sea level, and astronomical tide were extracted for a window of 2.5 days before and after the moment of maximum wind speed u, to ensure that the entire storm is captured. An example of one selected storm event for one location is presented in Fig. 4. The time index is defined such that the peak wind speed u, which is the main driver of storm surge, occurs at $t = 0$. The time series of the residual surge were derived, being the difference between the sea level and astronomical tide at every time step (contrary to the skew surge, which compares the peak surge and tide non-simultaneously). From now on, we refer to the residual surge hydrograph as (storm) surge hydrograph.

For each selected storm event, we defined several storm characteristics, as illustrated in Fig. 4:

- u : Maximum wind speed during the selected storm in meters per second. The wind speed was derived from the wind stress using a Charnock constant (Charnock, 1955) of α=0.02, see Appendix A for more details. Note that the aim of this study is to analyze the shape of surge hydrographs, and therefore an exact derivation of the wind speed is not the main focus.
- r : Wind direction during the maximum wind speed u in degrees clockwise with respect to North.
- w : Maximum sea level within a window of one day before and after the maximum wind speed u, in meters above NAP (the Dutch reference system).
- s : Maximum residual surge height within a window of one day before and after the maximum wind speed u, in meters.
- φ : Tidal offset defined as the time difference in hours between the maximum residual surge height s and the nearest astronomical high-tide. Note: a positive φ means that s precedes the high water, like in the example in Fig. 4.
- D_s : Exceedance duration of the residual surge at a level of 50% of s, in hours. The 50%-level was chosen, because it is a good balance between being low enough to capture side peaks in the surge hydrograph, and being high enough to focus on duration of a significant surge height. A sensitivity analysis was performed to justify that the duration at the 50%-level is an appropriate choice and we have investigated the robustness of this choice (See Appendix B).

An overview of correlations between these storm characteristics is presented in Appendix C.

3.2. Storm clustering

To examine how various storm characteristics influence the shape of surge hydrographs, we clustered storm events based on some of these storm surge characteristics. Different clustering approaches have been explored, including manual clustering based on physical drivers, as well as various data-driven techniques such as K-Means and Self-organizing maps. However, in this paper we focus on manual clustering based on physical drivers that potentially affect storm surge hydrographs.

The clustering procedure is illustrated in Fig. 5. Firstly, storms were clustered based on wind direction r, by defining 16 sectors of 22.5° wide (e.g. the northern sector ranges from 348.75° to 11.25°N). The wind direction was considered as the first clustering feature because

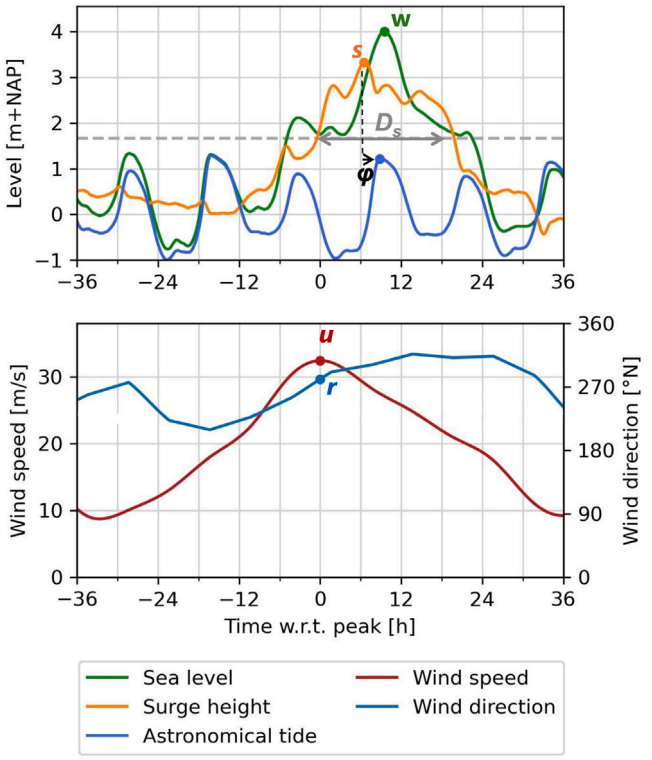

Fig. 4. Example of one selected storm event, including definitions of storm surge characteristics that play a role in this study.

it strongly affects the residual surge, as becomes clear in Fig. 5(a): This wind rose shows the distribution of s for storms corresponding to each wind direction sector. It can be seen that the highest residual surges are mostly caused by storms from wind directions W (270°N) and WNW (292.5°N). To illustrate the clustering procedure in this example, we select storms corresponding to wind direction WNW. Secondly, storms were clustered based on the tidal offset φ, since there is a strong interaction between tide and storm surge, which is further elaborated in Section 4. We expect that this interaction between tide and surge affects the shape of the surge hydrographs, and therefore we use φ as the second clustering feature. It can be observed in Fig. 5(b) that the tidal offset is very non-uniformly distributed. This observation is further explained in Section 4. The figure also shows that three values of the tidal offset appear to be the most dominant (the same holds for the other locations, as shown in Appendix D). Therefore, the storms corresponding to each wind direction sector are further subdivided into three clusters based on these dominant tidal offsets (±0.51 h), as indicated by the black and red squares in Fig. 5(b) (see Table 2 for an overview of these dominant values per location). In this example, we continue with the storm cluster corresponding to r=WNW and φ=1.5 h. Storms that fall outside these three bins are neglected in further analyses. Thirdly, storms are clustered based on their surge exceedance duration D_s, since the duration determines the 'width' of the surge hydrograph, and therefore largely affects its shape. Three equally-sized clusters are created based on the surge duration (storms with short, medium and long duration), as shown in Fig. 5(c). In this example, we select storm events corresponding to r=WNW, φ=1.5 h and a short surge duration. The clustering procedure results in groups of storm events for which we analyzed the storm surge hydrographs and defined a representative surge hydrograph per storm cluster. The set of surge hydrographs corresponding to the storm cluster of this example is shown in Fig. 5(d). Note that the surge exceedance duration D_s is only used as a clustering feature. The full storm time series is then used for the analysis of surge hydrographs (time series are not truncated at the exceedance level of D_s).

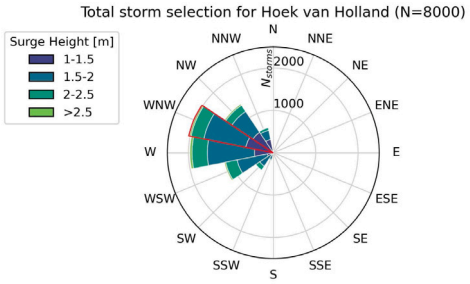

(a) Step 1: Clustering the 8,000 storm events into 16 wind direction sectors, based on r. In this example, storm events with r=WNW are selected.

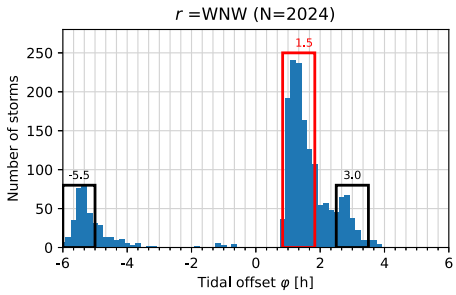

(b) Step 2: Sub-clustering the storm events corresponding to r=WNW into 3 clusters based on φ. In this example, storm events with $\varphi = 1.5 \pm 0.5$ h are selected.

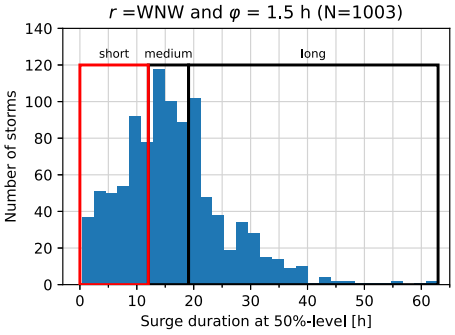

(c) Step 3: Sub-clustering the storm events corresponding to r=WNW and $\varphi = 1.5$ h into 3 clusters based on D_s. In this example, storm events with D_s=small are selected.

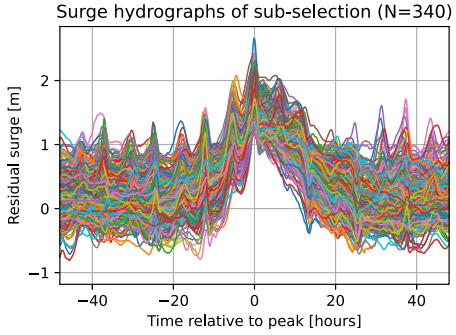

(d) Step 4: Select the storm surge hydrographs of the resulting storm sub-selection corresponding to r=WNW, $\varphi = 1.5$ h and D_s=small

Fig. 5. Illustration of the clustering procedure. In this example, the selection procedure for the storm cluster corresponding to location Hoek van Holland, wind direction r=*WNW*, tidal offset $\varphi = 1.5$ h and short wind exceedance duration D_s is shown.

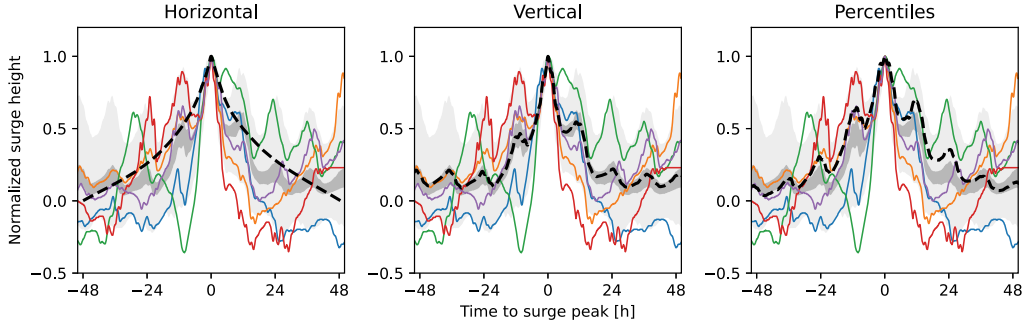

Fig. 6. Illustration of the application of different averaging methods for the storm surge hydrograph of a storm cluster with wind direction NW at location Vlissingen. The resulting, averaged hydrographs are shown as black, dashed lines. The contours of the storm cluster that is averaged are shown in gray color bands, for different percentiles of the data (the light gray band represents the 5th-95th percentile interval and the dark gray band represents the 40th–60th percentile interval). In colored lines some example storm surge hydrographs from the cluster are shown.

3.3. Storm surge hydrographs

The final step after clustering is to create an average storm surge hydrograph that represents the corresponding storm cluster. A common method for averaging is the so-called horizontal averaging, which consists of averaging the durations of individual storms at multiple (normalized) levels. This method is applied in the derivation of the design hydrographs of residual surge and wind speed in the current Dutch design guidelines (Chbab, 2015b) and in the study by Dullaart et al. (2023). The horizontal averaging method correctly accounts for the total number of hours in which the storm surge exceeds a specific level. However, this method has the disadvantage that the resulting hydrographs can become severely distorted, in particular for temporal patterns with distinctive side peaks, which is the case for the residual surge. As a result of horizontal averaging, all peaks are merged into one broad, smoothed peak, as illustrated in the graph to the left of Fig. 6. The figure shows the resulting averaged storm surge hydrographs as a black, dashed black line. The light gray color bands show the of the 5-95th-percentile interval, and the darker gray the contours of the 40th–60th percentile of the selected storms. In colored lines some individual storms from the cluster are plotted, as examples. Since merging of all side peaks to one broad peak leads to an unrealistic representation of the surge hydrograph, an alternative method to consider is vertical averaging: taking the vertical average over the individual storms at every instant of time. However, for vertical averaging it can be observed that it slightly underestimates the exceedance duration

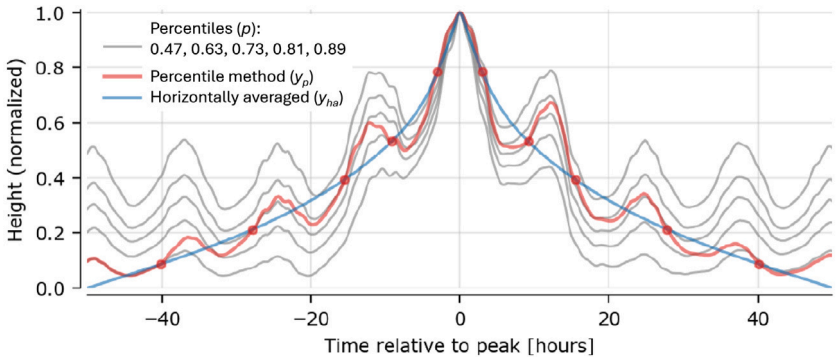

Fig. 7. Illustration of the percentile method. The gray lines show the surge hydrographs corresponding to different percentiles. For example, the lowest gray line corresponds, at every instant t, top = 0.47, the next gray line corresponds to 0.63, and so on (Geerse et al., 2019).

around the peak, especially for side peaks of the residual surge, as shown in the middle graph of Fig. 6. With regard to flood safety application, an underestimation of hydraulic loads is undesirable, as it is preferred to be conservative in design practice.

To overcome the pitfalls of the former averaging methods, we developed an alternative method to derive averaged storm surge hydrographs: the so-called percentile method (Geerse et al., 2019). This method is specifically useful for temporal patterns that are subject to the influence of a periodic signal (such as the tide), as is the case for hydrographs of the residual surge. The approach of the percentile methods is as follows: first the horizontally averaged durations are determined, yielding the blue line (y_{ha}) of Fig. 7. Next, a set of specific time instants relative to the peak are considered, that correspond to nodes in the pattern. These time instants (τ) are defined as factors of the tidal period (12.42 h): 1/4, 3/4, 5/4, 9/4, 13/4 (times 12.42 h). For a cluster of N normalized surge hydrographs, percentiles (0.01, 0.02, ...1.0) are calculated for all time instants τ. At time τ_i we now choose the percentile p such that it matches the height of the horizontally averaged pattern y_{ha}. That is, if we denote the percentile by y_p, we require that

$$y_{ha} = y_{p(\tau)}. \tag{1}$$

These percentiles y_p at time instants τ are illustrated by the red dots in Fig. 7. The resulting surge hydrograph from the percentile method results from interpolating the percentages (i.e. the p-values at time instants τ) for the time instants in between. This method preserves the oscillating pattern, while keeping – at least as an approximation – the same average horizontal durations (Geerse et al., 2019).

In Fig. 6 it can be observed that the percentile method provides a more representative, averaged storm surge hydrograph than the vertical and horizontal averaging methods. A similar conclusion results from Geerse et al. (2019), where it was stated that the percentile method ensures, at least approximately, that (1) the durations of residual surges and (2) time characteristics, such as secondary peaks, are well-represented. For these reasons, the percentile method was used within this study for averaging over storm surge hydrographs corresponding to a storm cluster.

4. Tidal offset

Before moving towards results concerning surge hydrographs, we briefly elaborate on observations based on an analysis of the tidal offset. The tidal offset φ is defined as the time (in hours) between the maximum residual surge and the closest astronomical high-tide. The offset is positive if the surge peak precedes the tidal peak, like in the example in Fig. 4. Fig. 8 shows histograms of the empirical distributions of the tidal offset derived from the selected SEAS5-WAQUA storm events, for clusters corresponding to three wind directions at Hoek van Holland. It can be seen that the tidal offset is very non-uniformly distributed and that the maximum residual surge hardly ever occurs during (astronomical) high tide. The fact that the distribution of the phase is strongly non-uniform has been observed in previous studies for the Dutch coast (Direktie Waterhuishouding en Waterbeweging, 1984; Janssen, 1990; De Ronde, 1985; Geerse, 2003; Chbab, 2015a), and also abroad (Horseburgh and Wilson, 2007). Horseburgh and Wilson (2007) presented the non-uniformity of the phase for stations along the East coast of England and Scotland, where it was also observed that the maximum of the surge rarely coincides with (astronomical) high tide. This non-uniformity is the result of interactions between surge and tide (Geerse, 2020; Horseburgh and Wilson, 2007): During storm surges, the relatively shallow North Sea becomes (slightly) deeper, and therefore the tidal wave propagates faster, resulting locally in a tide arriving sooner than the (predicted) astronomical tide. At the same time, wind stress is more effective at raising the sea surface in shallow water. The combined effect of these physical processes results in the non-uniform distribution of the tidal offset.

Table 2
Overview of the three observed, most dominant tidal offsets φ (in hours) per location. In the bottom row the tidal offsets as used in the current Dutch flood defense design guidelines are shown (Chbab, 2015a).

	Vlissingen	Hoek van Holland	Harlingen	Delfzijl
φ_1	2.5	1.5	1.333	1.833
φ_2	4.167	3.0	4.667	3.667
φ_3	6.0	−5.5	6.0	5.0
Current design practice	2.5	−4.5	5.5	5.5

Fig. 8 shows that roughly the same three values are most dominant for all wind directions (for this location 1.5, 3.0 and −5.5 h), but the frequencies of occurrence differ. For example, the occurrence of the tidal offset of 1.5 h is for the wind directions SSW and W more frequent than wind direction NNW. The empirical distributions of the tidal offsets for other locations are shown in Fig. D.20 of the Appendix D. All locations reveal three dominant phases (see Table 2) with varying frequency per wind direction. This information is valuable for future improvements of the design guidelines for coastal flood defenses, in which currently only a single value of the tidal offset is applied per location (Chbab, 2015a). These values are shown in the bottom row of Table 2.

A comparison with observations by Chbab (2015b) shows that the empirical distributions obtained from simulation data show approximately the same features for most locations, but also some discrepancies were noted (Geerse et al., 2019). For example, in observations, a tidal offset of about −4.5 h appeared to be the most frequent at Hoek van Holland, whereas this value is almost absent in the simulated data.

5. Storm surge hydrographs

In this section, we compare the shape of averaged, normalized surge hydrographs for different storm clusters at the four study locations. The

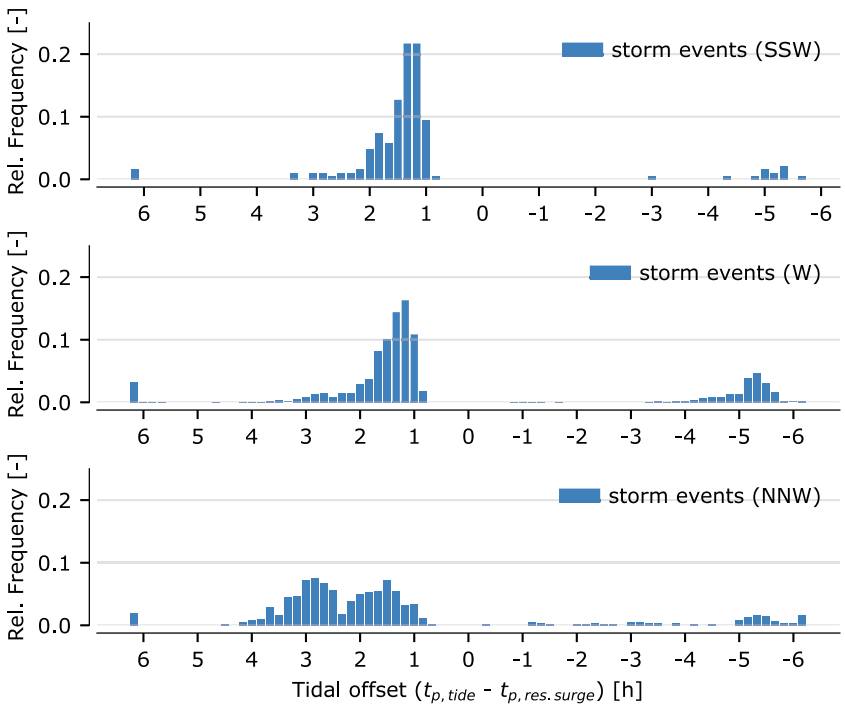

Fig. 8. Empirical distributions of the tidal offset φ in hours, for wind directions SSW, W and NNW at Hoek van Holland. The storm events, selected from the 8,000 extreme occurrences based on surpassing a sea level threshold (Table 1), are depicted in blue with a relative frequency. The offset is positive if the surge peak precedes the tidal peak.

aim is to identify storm characteristics that affect the shape of surge hydrographs and to derive a set of representative surge hydrographs that can be used in flood risk assessments for the Dutch coast.

5.1. Comparison of storm clusters

In Fig. 9 storm surge hydrographs are shown, representing storm clusters corresponding to wind direction West, for each coastal location. Surge hydrographs corresponding to the three dominant tidal offsets are indicated by different colors. The transparent lines show the variation between short (33% shortest) and long (33% longest) durations. The solid lines show the surge hydrographs corresponding to the medium duration class (33%–67%). The figure reveals that storms corresponding to different tidal offsets show different surge hydrographs, since the colored lines deviate from each other, especially for the coastal locations of Hoek van Holland and Delfzijl. Note that also variations due to different surge duration classes are substantial around the duration of the 50th percentile of the surge height. Next, we compare storm surge hydrographs for three wind directions at each coastal location, in Fig. 10. Again, the transparent lines show the variation between the short and long duration classes. From these graphs it can be observed that the different wind directions show similar storm surge hydrographs. However differences between the different duration classes are still substantial.

When comparing the four locations, it can be observed that each location has its particular storm surge hydrographs, which are characterized by interactions with the local tidal signal. For instance, the tidal signal at Hoek van Holland is asymmetric around the horizontal axis (see gray dashed line in Fig. 12(a)), which causes the multiple side peaks in the storm surge hydrograph.

Summarizing, the figures in this paragraph show that clustering based on location, tidal offset and exceedance duration is important for the shape of the resulting averaged storm surge hydrograph. Clustering based on wind direction is not important for the shape of the storm surge hydrograph, however it is important for the statistics of extreme wind speed and surge height. Westerly wind directions have a larger probability for extreme surge heights than easterly wind directions. This is visible in the wind rose of Fig. 5(a) and scatters in Fig. C.19 in Appendix C.

5.2. Comparison of surge magnitudes

In this section, we further subdivide the clusters based on the magnitude of the maximum surge height before normalizing and averaging. The objective is to investigate whether the most extreme storms (in terms of maximum residual surge height) show similar storm surge hydrographs as other, less extreme storms. Fig. 11 shows these averaged, normalized storm surge hydrographs for Hoek van Holland. Each figure represents a storm cluster based on wind direction West and a tidal offset φ of 1.5 h and surge duration class D_s. Results are presented for all three duration classes: the 33.3% shortest storms (upper graph), the 33.3% medium duration storms (middle graph) and the 33.3% storms with longest surge duration (lower graph). Within each graph, storms are further subdivided based on the magnitude of the surge peak s, as indicated by the different colored lines. The subdivision is done by defining surge values that divide the storm data into four equally-sized clusters (before sub-clustering based on duration): $1 < s < 1.5$, $1.5 < s < 1.7$, $1.7 < s < 2.0$ and $2 < s < 3$ m. This is done to ensure that each sub-cluster based on surge magnitude is approximately equal in size.

It can be seen that the storm surge hydrographs look very similar for different magnitudes of the maximum surge height. This implies that it is possible to consider the same storm surge hydrographs for any magnitude of the peak (within a cluster based on wind direction, tidal offset and exceedance duration class of the surge). We call this the ‘scaling property’: the storm surge hydrograph can be scaled to any surge height s, which makes it very suitable for design calculations. However, this property is only valid after performing the above-mentioned clustering steps.

One may observe from Fig. 11 that the number of storms N within the different surge peak magnitude sub-clusters differs per duration class (the three graphs). In the sub-cluster with surge heights between 2 and 3 meters (red lines), N is smaller in the lower graph, compared to the other middle and upper graphs. Similarly, the number of storms

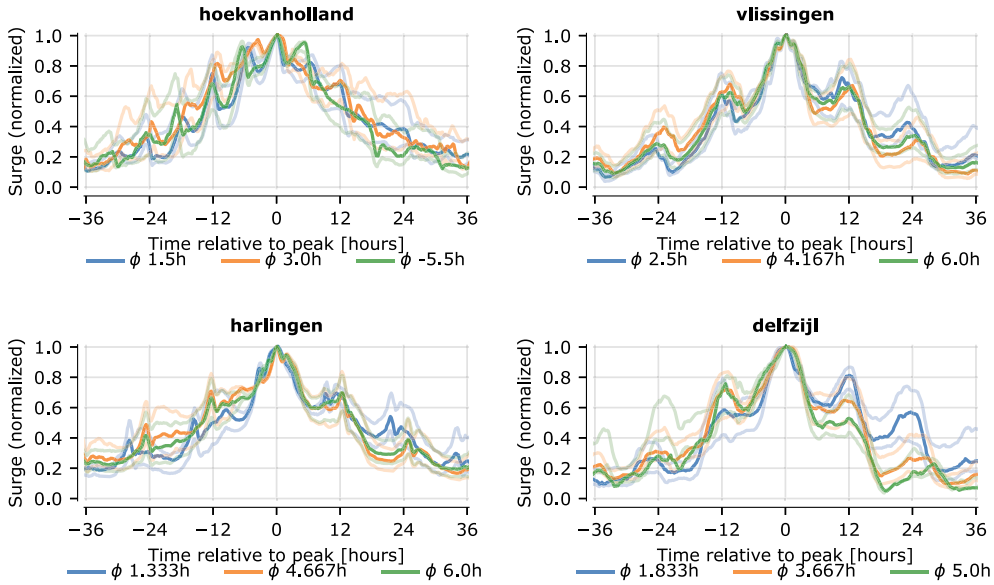

Fig. 9. Normalized storm surge hydrographs for the three dominant tidal offsets and wind direction West. The transparent lines show the variation between the short and long durations. The solid lines show the medium duration class (33%–67%).

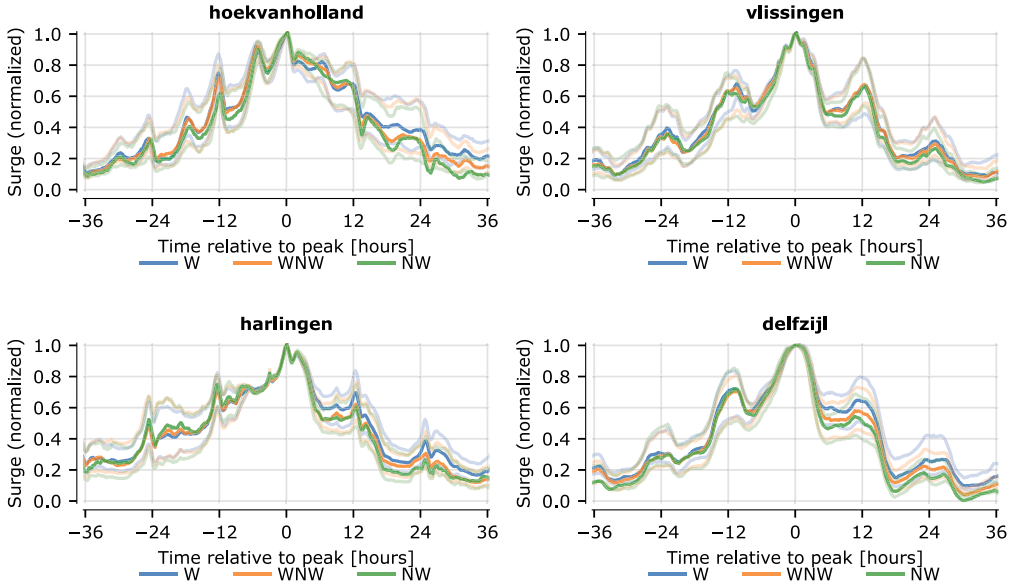

Fig. 10. Normalized storm surge hydrographs for three dominant wind directions for the most dominant tidal offset. The transparent lines show the variation between the short and long durations. The solid lines show the medium duration class (33%–67%).

in the sub-cluster with surge heights between 1 and 1.5 meters (blue lines) is largest in the lower graph. These observations are related to the definition of the surge exceedance duration s, as discussed in Appendix B. By definition, the exceedance duration of a relative surge level causes a negative correlation between s and D_s: For a storm with large surge magnitude s, the 50%-exceedance level is higher than for a storm with lower-magnitude s, and a higher level is generally exceeded for a shorter time duration. It is important to take this into account as soon as probabilities are assigned to the occurrence of each cluster with according storm surge hydrograph: the combination of an extreme surge height and a storm surge hydrograph with a long exceedance duration (of a relative level) should have a smaller probability than the extreme surge height with short exceedance duration. This is further elaborated in Geerse et al. (2022), Caspers and Kindermann (2023).

The storm surge hydrographs in Fig. 11 correspond to location Hoek van Holland, but the same can be observed for the other coastal locations. From Fig. E.21 in Appendix E it follows that the scaling property also holds for the other locations.

5.3. Comparison to current design practice

In the current Dutch design guidelines, called WBI, a single storm surge hydrograph is used for coastal flood defenses, which has a base duration of 44 h (Chbab, 2015b) and a fixed value for the tidal offset, varying per coastal area. In total, three coastal areas are distinguished. Fig. 12 shows the resulting sea level hydrograph according to WBI, compared to those following from this study. In Fig. 12(a), the resulting, normalized storm surge hydrographs for Hoek van Holland are shown for the three duration classes, for wind direction West and the most dominant tidal offset (1.5 h). The black, dashed line shows the trapezoidal surge schematization according to WBI. The resulting sea level hydrograph follows from scaling the storm surge hydrograph to a

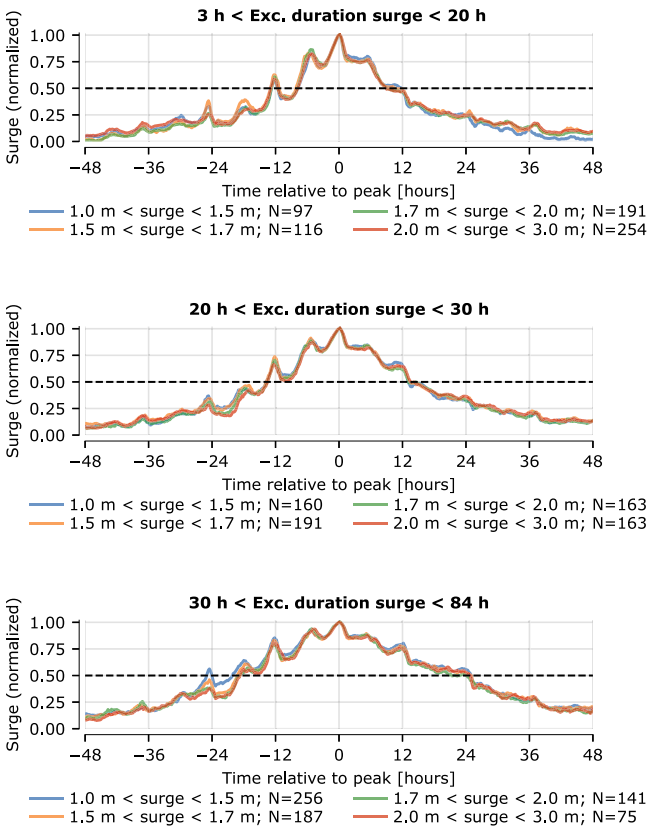

Fig. 11. Comparison of the averaged normalized storm surge hydrographs for different magnitudes of the residual surge peak, for Hoek van Holland, wind direction West and a tidal offset of 1.5 h.

value of 4.3 meters and combining it with the tidal signal by accounting for the tidal offset. This is shown in Fig. 12(b) for the storm surge hydrographs from Fig. 12(a) and in Figs. 12(c) and 12(d) for the other two dominant tidal offsets at Hoek van Holland. From this example, the variation in duration classes and tidal phases is evident, as discussed in Section 5.1. It appears that the sea level hydrograph according to WBI is most similar to the sea level hydrograph with a tidal offset of −5.5 h (Fig. 12(d)). This can be explained by the fact that a tidal offset of −4.5 h is applied in WBI (see Table 2). Besides, the WBI sea level hydrograph matches best with the short duration class (blue line in Fig. 12(d)). It can be seen that the other tidal offsets are more common for this locations (i.e. have larger amounts of storms N in the clusters), which implies that the WBI schematization does not give an accurate representation of the sea level hydrograph at Hoek van Holland. The same conclusions hold for other coastal locations. These graphs are shown in Fig. F.22 to Fig. F.24 of Appendix F. For example, the sea level hydrograph for Vlissingen with a tidal offset of 2.5 h shows strong similarities with the WBI hydrograph, for which also a value of 2.5 h is applied.

For the sea level hydrographs from Fig. 12 (and from the appendix for the other locations) we evaluate the exceedance duration of the sea level at different levels. The results are presented in Fig. 13 for the four locations. The exceedance durations for the current WBI schematization are depicted in red and in gray for the sea level hydrographs from different storm clusters of this study. The black line represents the combined average of the gray lines, by accounting for the likelihood of each gray line. The figure shows that the sea level hydrographs according to the current guidelines (in red) show a shorter exceedance duration in the flanks (at lower sea levels), compared to sea level hydrographs from the simulated data (in black). However, the duration of the peak varies per coastal location. For Hoek van Holland and Vlissingen, the WBI schematization gives a longer exceedance duration at the peak than the sea level hydrographs from this study, and vice versa for Harlingen and Delfzijl. Another important remark is that the variation in exceedance duration between the different sea level hydrographs in this study (gray lines) is largest for Hoek van Holland and Harlingen. This can be explained by the fact that the tidal signal is more asymmetric at these two location, when compared to the other two locations. Their tidal signals are shown by gray, dashed lines in Fig. 12 for Hoek van Holland and Fig. F.23 for Harlingen (compare to tidal signal in Fig. F.22 and Fig. F.24 of the other two locations).

6. Discussion

In this section, we discuss potential limitations and implications of this study.

6.1. Reliability of the data

The wind data are derived from SEAS5, the seasonal forecast product by ECMWF, and the corresponding water level data are simulated using WAQUA-DCSMv5, with the SEAS5 wind stress as input. We translate the SEAS5 wind stress to time series of wind speed, using a Charnock constant of 0.020, in order to achieve representative wind speeds that are in line with the wind statistics that are currently applied in Dutch design guidelines for coastal flood (Geerse et al., 2022). However, as can be seen in Fig. A.14, it is difficult to determine a suitable Charnock value and at the same time the choice has a large effect on the obtained wind speeds, up to several meters per second for Charnock values commonly used in the literature. However, it is important to note that this study focuses on storm surge hydrographs, and the residual surge from WAQUA is insensitive to the choice of the Charnock value, since the WAQUA simulations are based on the original wind stress from ECMWF.

Regarding the absolute values of the residual surge, recent research by de Valk and van den Brink (2023) has shown that a bias correction of 10% is required for the SEAS5 wind stress input in WAQUA, to result in representative surge heights for the Dutch coast. This bias correction, however, is not yet implemented in the version of the data that is used within this study. While the exact magnitudes of the wind speeds and residual surges presented in this study are therefore subject to some uncertainty, the normalized storm surge hydrographs and observed trends in the correlations are insensitive for this bias correction. Consequently, the key conclusions remain valid even if the absolute peak values deviate.

6.2. Clustering approach

In this study, we present results for a clustering procedure based on three storm characteristics (wind direction, tidal offset and surge duration). In addition, we analyzed the effect of clustering storms based on the surge magnitude, but this did not affect the resulting shape of the hydrograph. We presume that the three considered storm characteristics are dominant in determining the shape of surge hydrographs. However, other storm characteristics, may be of importance for the resulting shapes of surge hydrographs. Alternatively, the clustering could be performed based on the entire surge time series, using data-driven methods such as K-Means, without defining storm characteristics first. This approach, among others, is currently being investigated in a separate study.

There is substantial natural variability in storm surge time series – as illustrated by the confidence bands in Fig. 6 – which results in uncertainty of the resulting representative surge hydrographs. Since each cluster is summarized into one representative normalized surge hydrograph using an averaging method, the variability within the hydrographs is largely reduced. Consequently, minor adjustments to the sectors, bins or classes in the clustering process have a limited effect

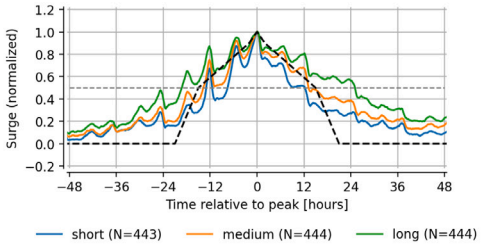

(a) Normalized storm surge hydrographs (φ = 1.5h)

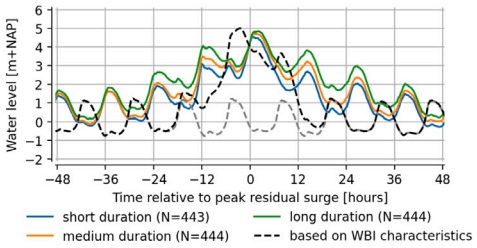

(b) Sea level hydrographs ($\varphi = 1.5$h)

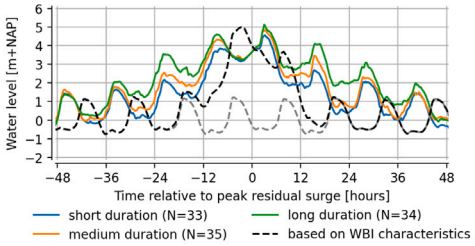

(c) Sea level hydrographs ($\varphi = 3.0$h)

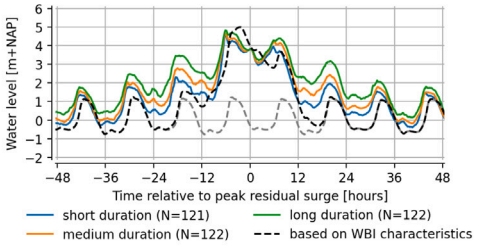

(d) Sea level hydrographs ($\varphi = -5.5$h)

Fig. 12. Normalized storm surge and sea level hydrographs for location Hoek van Holland, corresponding to a maximum surge height s of 4.3 m, compared to the WBI schematization (black, dashed lines). The corresponding astronomical tide is depicted as a gray dashed line. The sea level hydrographs are presented for wind direction West and the three dominant tidal phases φ. The three colors represent the three duration classes (short, medium, long).

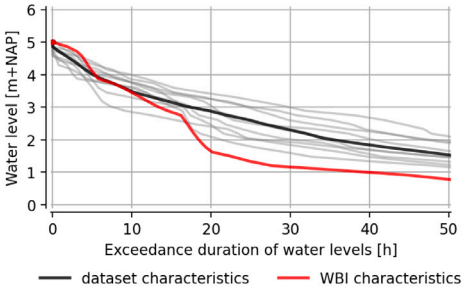

(a) Hoek van Holland (maximum residual surge height s 4.3 m)

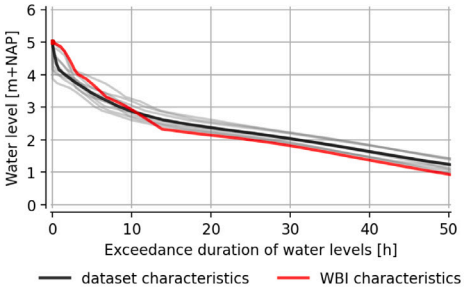

(b) Vlissingen (maximum residual surge height s 3.0 m)

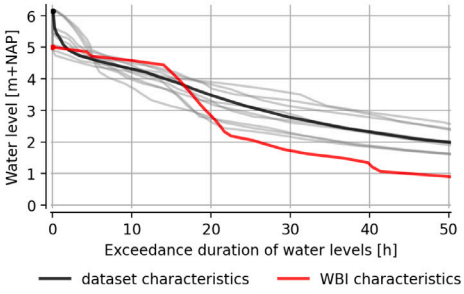

(c) Harlingen (maximum residual surge height s 5.3 m)

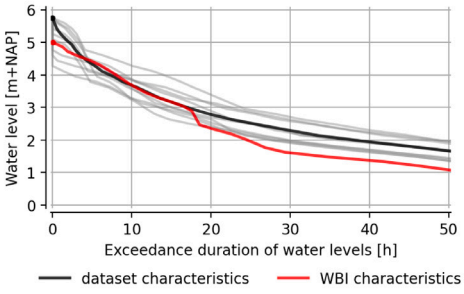

(d) Delfzijl (maximum residual surge height s of 4.5 m)

Fig. 13. Exceedance duration in hours for different sea level hydrographs. The y-axes represent different levels of the sea level and the x-axes represent the amount of hours that the sea level exceeds the corresponding sea level, for different sea level hydrographs. The red lines show the exceedance durations for the sea level hydrographs according to WBI, the gray lines for nine characteristic sea level hydrographs from this study (3 tidal offsets x 3 duration classes) and the black line shows the weighted average for these nine scenarios.

on the overall results, as each cluster includes a large number of storm events. This is for example illustrated by analyzing the sensitivity of resulting surge hydrographs to the choice of definition of storm surge duration at the 50%-level of s, which appeared to have a very limited impact (see Appendix B). Still, choices made in clustering – such as the wind direction sectors (±12.25°), tidal offset bins (±0.5 h), and duration classes (based on 33% percentiles) – influence the number of storm events within each cluster. As a result, some degree of uncertainty is inherent in the clustering process.

6.3. Climate change

The surge hydrographs that were derived in this study are representative for hydraulic loads in current climate. However, most flood defenses in the Netherlands are being designed for a lifespan of more than 50 years. Sea level rise is then taken into account within sea level statistics that are used to scale surge hydrographs to design water levels (as shown in Fig. 12). However, other effects, such as changing storm climate and interactions between sea level rise and storm surge, are not considered. We recommend to study surge hydrographs and the effect of climate change, based on data from climate models for future scenarios, such as the KNMI'23 climate scenarios (Van Dorland et al., 2023).

6.4. Storm selection window and multiple-peaked storms

During the analysis of the storm surge hydrographs, it appeared that the storm surge hydrographs sometimes exhibit a second storm surge peak on the edges of the considered time window. When averaging the storm surge hydrographs and normalizing by the peak at $t = 0$ for a certain selection, it happens that the second surge peak ($t \neq 0$) becomes larger than 1. This suggests that the time window of three days that we have applied to select independent storm events in the POT may be too short. We did not systematically test alternative windows. Since the choice of the time window length may influence the results, we recommend to perform a sensitivity analysis to evaluate the effect of this selection window on the resulting surge hydrographs, before using the resulting hydrographs in design practice.

These second peaks are probably the result of two or more storms occurring shortly after each other, so called twin storms. Multiple-peaked storms have been observed several times at the Dutch coast in the past, with the most recent event in 2022, when the storms Dudley, Eunice and Franklin occurred shortly after each other and caused substantial storm surges (Zijderveld et al., 2022). Multiple-peaked storms can pose an additional risk to flood defense infrastructure, since they can result in further damage, while there is no time for repair after the first storm event. We recommend to further study the characteristics of these multiple-peaked storms and to propose a representative storm surge hydrograph for multiple-peaked storms, that can be used in design practice.

6.5. Relevance

One of the main observations from the analysis of extreme storms from the large synthetic dataset is that storm surge hydrographs of extreme storms reveal different shapes than the one currently proposed in the Dutch design guidelines for coastal flood defenses that are based on observations, which contain a limited amount of extreme storms. We applied a novel method for averaging over storm surge hydrographs within a cluster, called the percentile method, in order to preserve sufficient detail as well as a correct duration of the storm surge hydrograph, which can explain the observed differences. Comparisons of the averaged storm surge hydrographs with those prescribed in current guidelines revealed that the latter typically yields shorter durations in the flanks. Differences in exceedance durations around the peak varied by location, indicating that the newly proposed hydrographs may exhibit longer or shorter exceedance durations depending on the specific location.

Moreover, the current guidelines suggest one value for the time offset between the peak of the storm surge and astronomical high tide. Based on the synthetic dataset, three values appear to be dominant for each location. The two observed, extreme storms as presented in Fig. 1 exhibited a time offset of 2 and 1.5 h respectively. The current guidelines suggest a value of −4.5 h for Hoek van Holland, while we concluded from the synthetic data that 1.5 h is the most dominant value (followed by 3.0 and −5.5 h), which is more in line with the observed tidal offsets as described in the Introduction. Although these are only two observations, the results suggest that the currently applied, fixed values of the tidal offsets may not be representative for extreme storms along the Dutch coast.

Storm surge hydrographs and tidal offsets are applied in safety assessments of current flood defenses and in design for flood defense reinforcements, which are based on the estimation of annual failure probabilities. The effect of different storm surge hydrographs and tidal offsets on resulting estimated failure probabilities of coastal flood defenses should be investigated, which also includes models of time-dependent simulation of damage. Some first analyses were made in Caspers and Kindermann (2023).

7. Conclusions

This study presents a detailed analysis of characteristics and surge hydrographs associated with extreme storm events affecting the Dutch coastal area, based on a large dataset of simulated time series for wind and sea levels. A total of 8,000 storm events were selected for each of the four study locations and parameterized using various storm characteristics.

An analysis of the tidal offset revealed a strong non-uniform distribution, consistent with previous studies, which can be explained by interactions between tide and surge. For each location, we identified three dominant values of the tidal offset, with varying probabilities based on wind direction. For comparison, the current, Dutch design guidelines use one fixed tidal for each location. This finding supports the need for revising the current design guidelines for coastal flood defenses, to account for natural variability due to tide-surge interactions.

From analyses of storm surge hydrographs for different storm clusters it appeared that the location, tidal offset and the surge duration affect the shape of the storm surge hydrograph, resulting in different representative surge hydrographs. We also clustered based on wind direction, since this is relevant for corresponding probabilities of wind speed and surge magnitudes. However, we concluded that for *shape* of storm surge hydrographs, clustering based on wind direction is not important. By clustering storms for different magnitudes of the surge height, we observed that the averaged storm surge hydrographs can be scaled to any surge height within the corresponding cluster (by taking the probabilities into account), which makes the hydrographs very suitable for design calculations.

The resulting surge hydrographs, combined with the three dominant tidal offsets, were used to generate representative sea level hydrographs for each cluster and location. These sea level hydrographs were compared to those from current design guidelines, in terms of exceedance durations of sea levels. The comparison revealed that the sea level hydrographs from current guidelines tend to have shorter durations on the flanks of the hydrograph. Around the peak, the sea level hydrographs derived from simulated data show considerable variability in duration, primarily influenced by the tidal offset. This suggests that using a single, fixed surge hydrograph and tidal phase in the current guidelines may not fully capture the natural variability during extreme storm surge conditions.

This study provides valuable insights that can be used to improve the description of hydraulic loads in the design guidelines for coastal

flood defenses in the Netherlands. The outcomes suggest that not only the magnitude (and direction) of wind speed and surge height, but also storm duration and timing with respect to the tidal cycle, are important factors for deriving surge hydrographs, and therefore characterizing extreme sea levels. Before integrating these factors into design guidelines, further research is needed to assess whether their inclusion significantly affects the flooding probabilities derived from reliability assessments of coastal infrastructure.

CRediT authorship contribution statement

Jochem J. Caspers: Writing – review & editing, Writing – original draft, Visualization, Validation, Software, Resources, Project administration, Methodology, Investigation, Funding acquisition, Formal analysis, Data curation, Conceptualization. **Paulina E. Kindermann:** Writing – review & editing, Writing – original draft, Visualization, Validation, Software, Resources, Methodology, Investigation, Funding acquisition, Formal analysis, Data curation, Conceptualization. **Guus W.F. Rongen:** Writing – review & editing, Visualization, Validation, Supervision, Software, Resources, Project administration, Methodology, Investigation, Funding acquisition, Formal analysis, Data curation, Conceptualization. **Chris P.M. Geerse:** Validation, Supervision, Methodology, Investigation, Funding acquisition, Formal analysis, Conceptualization.

Declaration of Generative AI and AI-assisted technologies in the writing process

During the preparation of this work the authors used Chatgpt in order to improve language and readability. After using this tool, the authors reviewed and edited the content as needed and take full responsibility for the content of the publication.

Declaration of competing interest

The authors declare the following financial interests/personal relationships which may be considered as potential competing interests: Paulina Kindermann reports financial support was provided by Rijkswaterstaat Water Traffic and Living Environment. If there are other authors, they declare that they have no known competing financial interests or personal relationships that could have appeared to influence the work reported in this paper.

Acknowledgments

This research was conducted within the Kennis voor Keringen (KvK) program, a research program on flood defenses and their threats financed by Rijkswaterstaat, the ministry of Infrastructure and Water Management in the Netherlands. The data for the study were provided by KNMI. The authors would like to thank the editors and the anonymous reviewers for their valuable insights during the review process.

Appendix A. Wind stress to wind speed

In this study, wind speed is derived from surface stress rather than using ECMWF wind speed directly, as the latter exhibits much lower extremes compared to measurement-based statistical analyses (left column in Fig. A.14). A Charnock relation (Charnock, 1955) is used to convert the surface stress from the ECMWF-model to wind speed (based on a logarithmic wind profile). This appendix supports the decision to convert the surface stress to a wind speed.

To show the effect using different values of the Charnock parameter α_{ch}, the wind statistics after calculating wind speed from surface stress are shown in Fig. A.14. The measurement-based statistics used in the Dutch design guidelines (WBI) for each coastal station are shown in red. Note that these are the statistics *without* integrated statistical uncertainty. The blue dots indicate the empirical exceedance frequencies plotted with plotting positions a=0.3 and b=0.4.

The slope of the calculated wind speeds from ECMWF-surface stress decreases for higher wind speeds, compared to the slope from the WBI-statistics. The wind used for the derivation of the WBI-statistics is *potential* wind speed, related to the roughness of grass. Since the ECMWF-model is above open water (with a lower roughness), it should be higher than the wind speed in the Dutch design guidelines. Because of this, and since the highest wind speeds are the most relevant ones in this study, a Charnock-parameter of 0.020 was chosen.

Appendix B. Sensitivity analysis surge duration

In this study, we have defined the surge duration as the exceedance duration of the level at 50% of the maximum surge height s during a storm. This choice may seem arbitrary and therefore we have analyzed the effect of exceedance level on the resulting surge hydrograph shapes in the surge duration clusters. For this sensitivity analysis, we analyzed four different definitions of the surge duration D_s, two relative levels (with respect to surge peak) and two absolute levels: the exceedance duration of 50% of s, 75% of s, 0.5 m and 1.0 m, as defined in Fig. B.15, By definition, exceedance durations of relative levels correspond to a slight negative correlation between D_s and s, as illustrated in Fig. B.16: the exceedance level lies higher for storms with high s, and high levels generally have shorter exceedance durations. On the other hand, exceedance durations of absolute levels have a positive correlation with the surge height s: the higher the maximum surge, the longer a low surge level (0.5 or 1 m) is generally exceeded, which can be seen in the lower two plots of Fig. B.16.

The exceedance duration D_s is a result variable in this study and calculated for all 8,000 storm events selected by peak-over-thresholds. The variable D_s is used to cluster storms into three groups: short (33% shortest), medium (33%–67%) and long (33% longest) durations. For each group we derive a representative surge hydrograph. To analyze the effect of the definition of D_s on these resulting, representative surge hydrograph, we follow the methodology for all four definitions of D_s. Fig. B.15 shows a comparison of the resulting surge hydrographs for the four definitions of D_s, for storms corresponding to wind direction WNW (292 °N) for three duration classes (short, medium and long). The figure reveals that the resulting surge hydrographs do not respond strongly to the definition of D_s. In Fig. B.18 the normalized surge hydrographs show similar shapes for each duration cluster. A distinct exception is the resulting surge hydrograph with short duration when defining D_s as the exceedance of the 75%-level of s. This level is rather high in the surge hydrographs and some secondary peaks of the hydrographs will be lower than this level, which results in very short durations. This also explains the small side peaks of the narrow histogram (orange) in Fig. B.17. Generally speaking, the relative level of 50% seems an appropriate choice for the definition of D_s and a different definition would not have significantly altered the results of this study.

Appendix C. Correlations between storm characteristics

Appendix D. Distribution of tidal offsets

Appendix E. Storm surge hydrographs

Appendix F. Sea level hydrographs

See Figs. F.22–F.24.

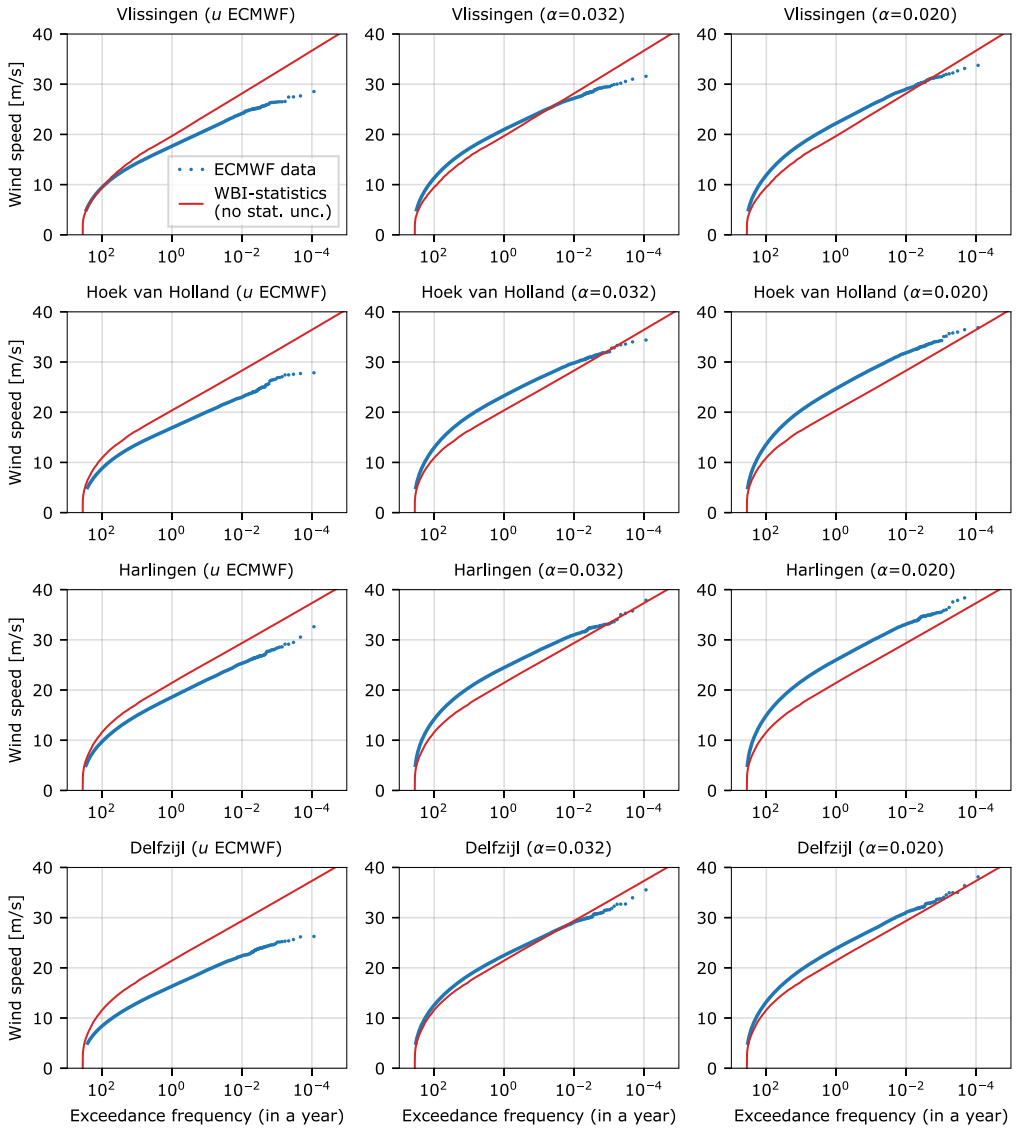

Fig. A.14. Comparison between wind statistics for the original ECMWF wind statistics (left) and different Charnock-parameter values (center α_{ch}=0.032, and right α_{ch}=0.020).

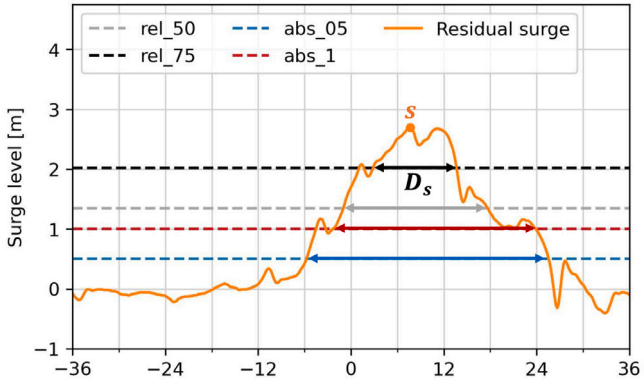

Fig. B.15. Four different definitions of D_s: In gray the exceedance duration of the level at 50% of the maximum surge height s (chosen in this study), in black of the level at 75% of s, in red the exceedance duration of 1 m surge and in blue of 0.5 m surge.

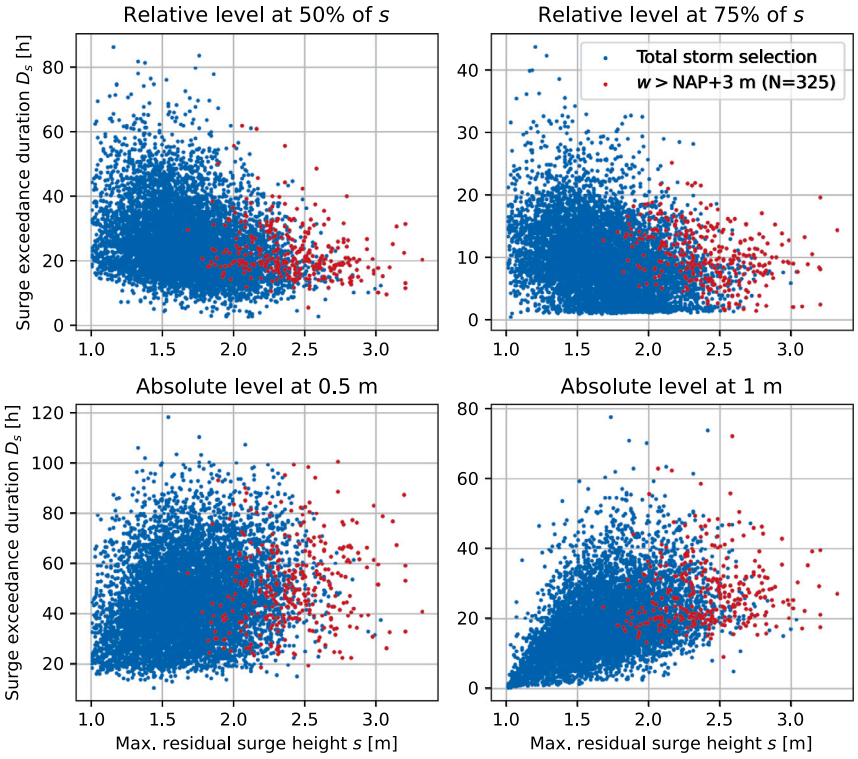

Fig. B.16. Comparison of the correlation between exceedance duration D_s and maximum surge height s of a storm, for four different definitions of D_s, as illustrated in Fig. B.15.

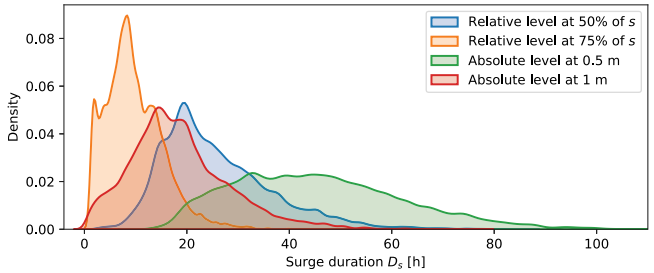

Fig. B.17. Comparison of histograms of exceedance duration D_s, for four different definitions of D_s, as illustrated in Fig. B.15.

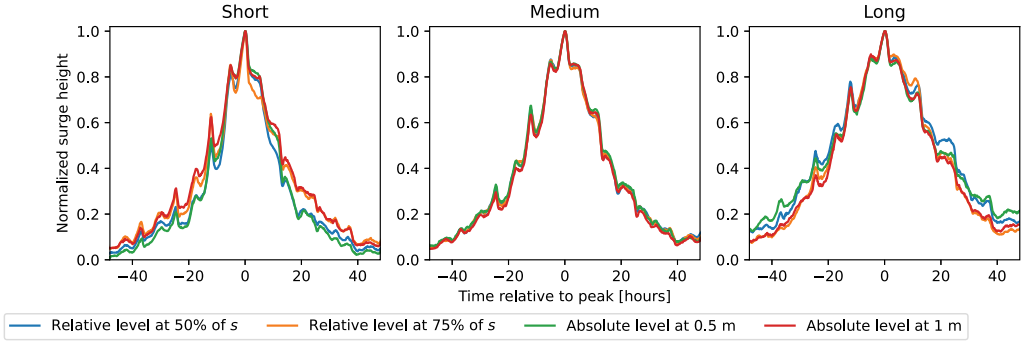

Fig. B.18. Comparison of resulting surge hydrographs for four different definitions of D_s for wind direction WNW, where storms were subdivided into three duration clusters, based on D_s: short, medium and long storms.

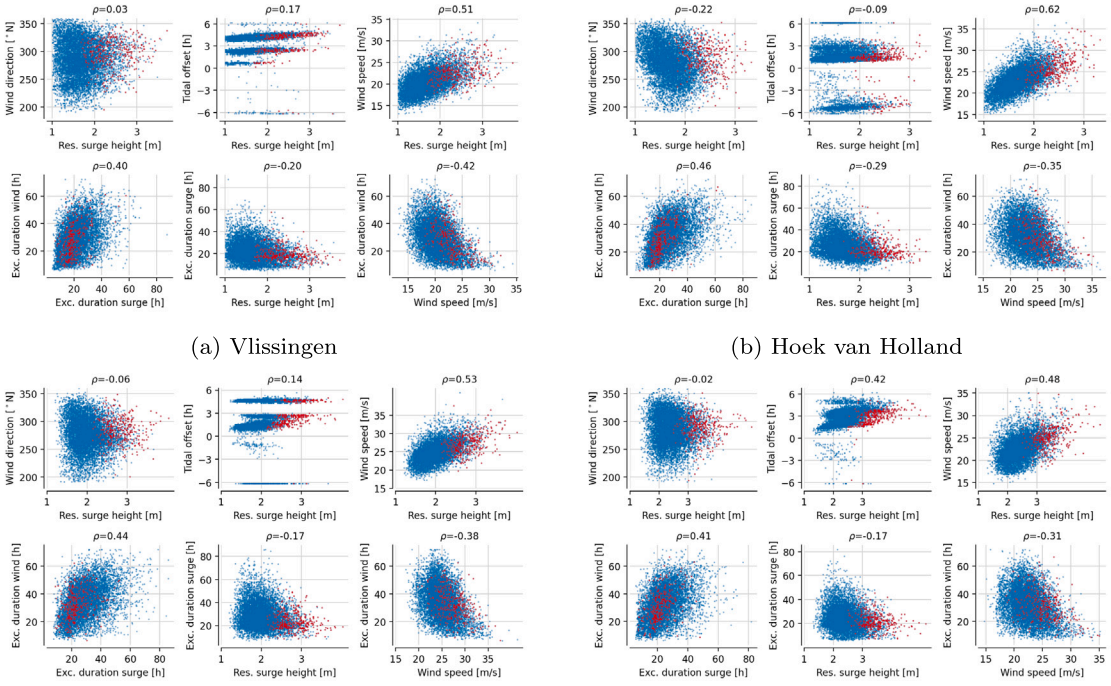

(a) Vlissingen

(b) Hoek van Holland

(c) Harlingen

(d) Delfzijl

Fig. C.19. Scatter plots for different combinations of storm characteristics. In blue for the total selection of 8,000 storms, and in red for storm events that exceed a sea level of NAP+3 m. The subtitles show Pearson's correlation coefficient.

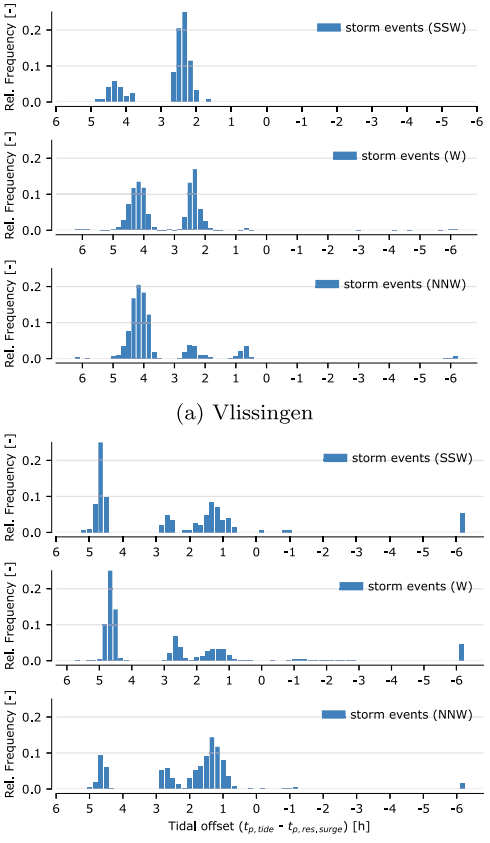

(a) Vlissingen

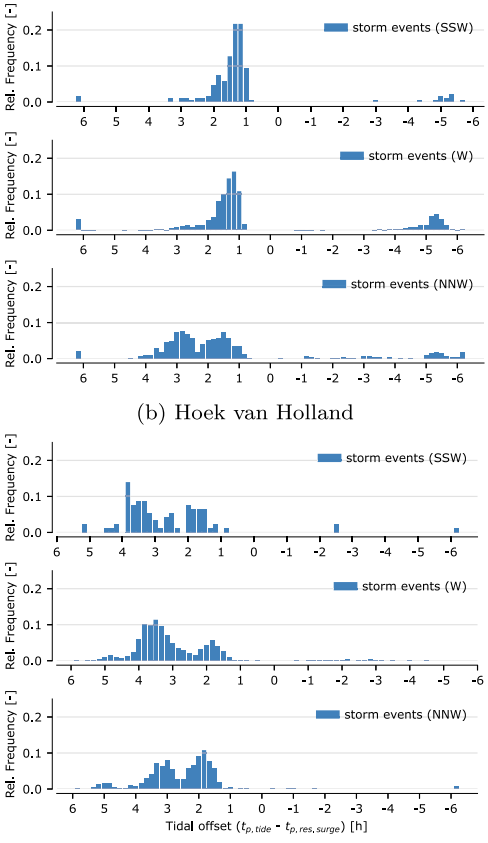

(b) Hoek van Holland

(c) Harlingen

(d) Delfzijl

Fig. D.20. Empirical distributions of the tidal offset φ [h], for wind directions SSW, W and NNW for the four coastal stations. In blue for the 8,000 selected storm events and in red for storms resulting in a sea level that exceeds NAP+3 m.

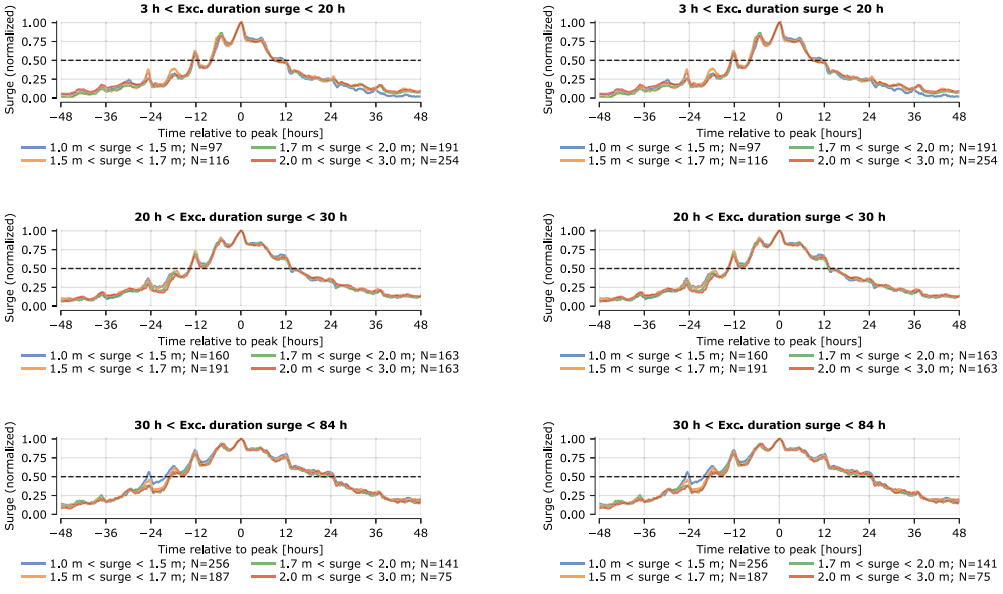

(a) Vlissingen (tidal offset $\varphi = 4.167$ h)

(b) Hoek van Holland (tidal offset $\varphi = 1.5$ h)

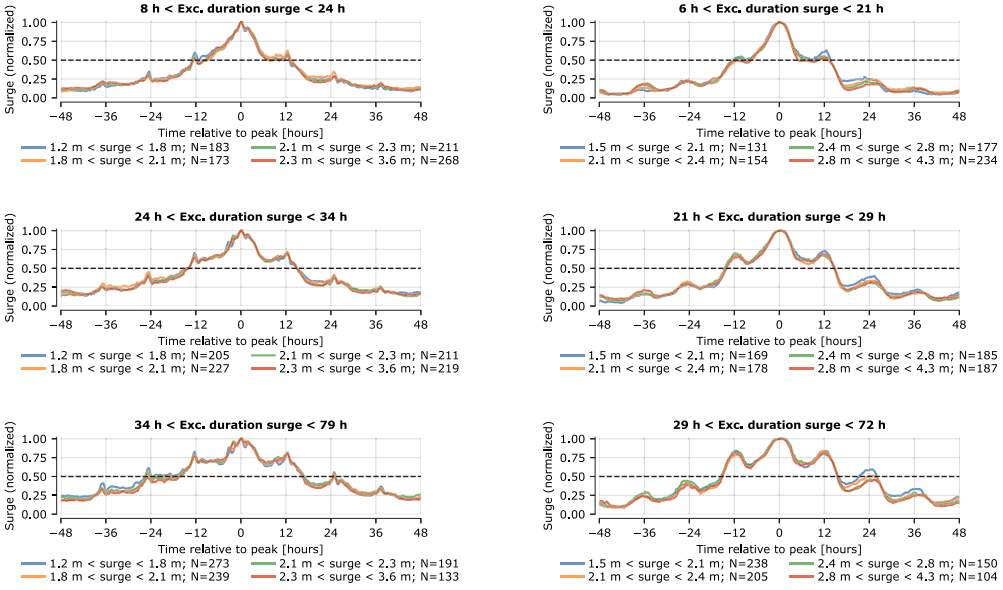

(c) Harlingen (tidal offset $\varphi = 4.67$ h)

(d) Delfzijl (tidal offset $\varphi = 3.67$ h)

Fig. E.21. Comparison of averaged, normalized storm surge hydrographs for different magnitudes of the maximum surge height s (different colors) for the three surge duration classes (subplots), for four coastal stations (a to d), wind direction West and the most dominant value of the tidal offset.

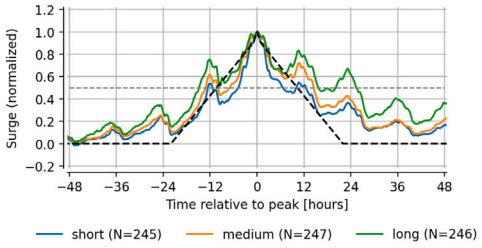

(a) Storm surge hydrographs ($\varphi = 2.5$ h and direction West)

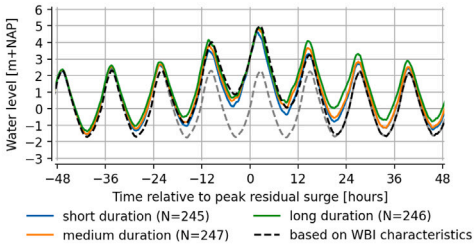

(b) Sea level hydrographs ($\varphi = 2.5$ h and direction West)

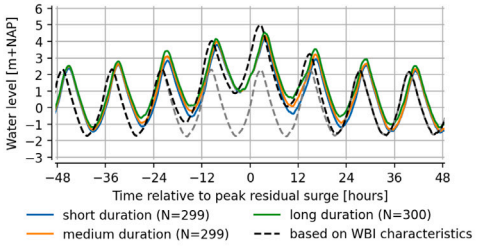

(c) Sea level hydrographs ($\varphi = 4.167$ h and direction West)

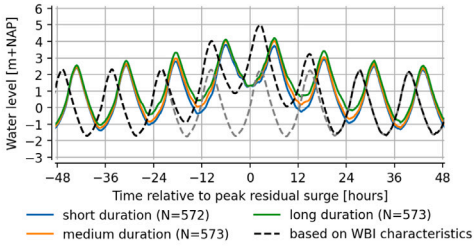

(d) Sea level hydrographs ($\varphi = 6.0$ h and direction West)

Fig. F.22. Normalized storm surge and sea level hydrographs for location Vlissingen, corresponding to a maximum surge height s of 3.0 m, compared to the WBI schematization (black, dashed lines). The corresponding astronomical tide is depicted as a gray dashed line. The sea level hydrographs are presented for direction West and the three dominant tidal phases. The three colors represent the three duration classes (short, medium, long).

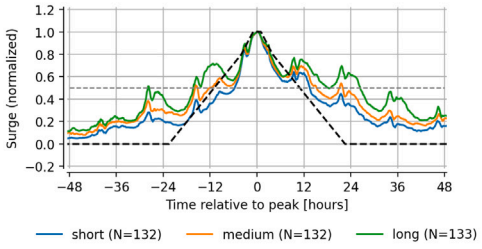

(a) Storm surge hydrographs ($\varphi = 1.33$ h and direction West)

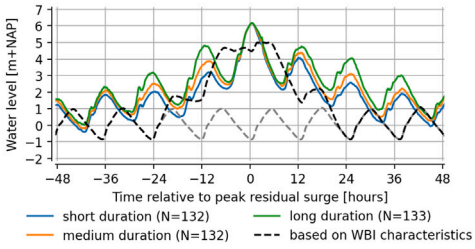

(b) Sea level hydrographs ($\varphi = 1.33$ h and direction West)

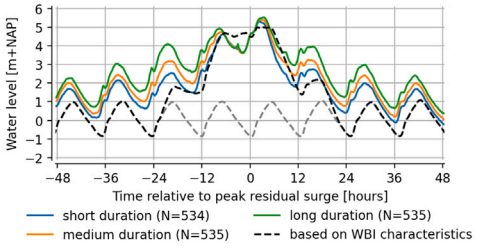

(c) Sea level hydrographs ($\varphi = 4.67$ h and direction West)

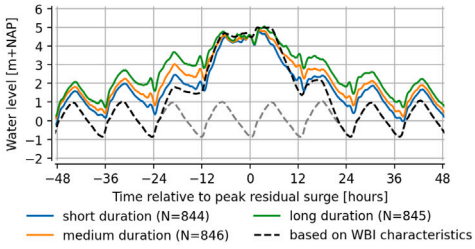

(d) Water level ($\varphi = 6.0$ h and direction West)

Fig. F.23. Normalized storm surge and sea level hydrographs for location Harlingen, corresponding to a maximum surge height s of 5.3 meters, compared to the WBI schematization (black, dashed lines). The corresponding astronomical tide is depicted as a gray dashed line. The sea level hydrographs are presented for direction West and the three dominant tidal phases. The three colors represent the three duration classes (short, medium, long).

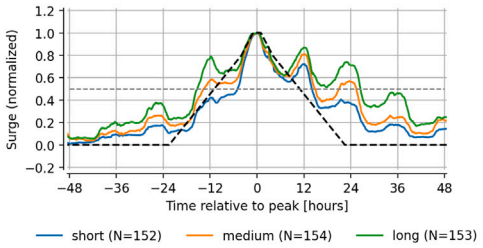

(a) Storm surge hydrographs ($\varphi = 1.83$ h and direction West)

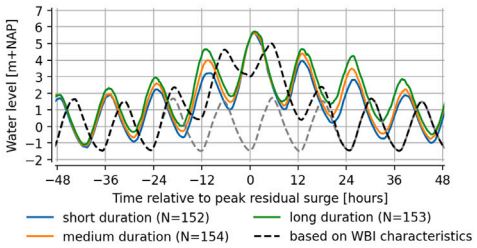

(b) Sea level hydrographs ($\varphi = 1.83$ h and direction West)

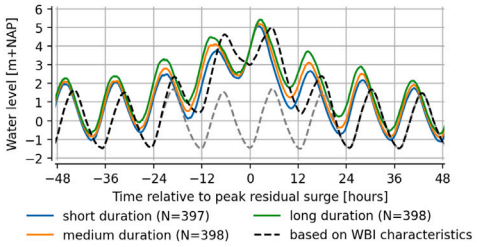

(c) Sea level hydrographs ($\varphi = 3.67$ h and direction West)

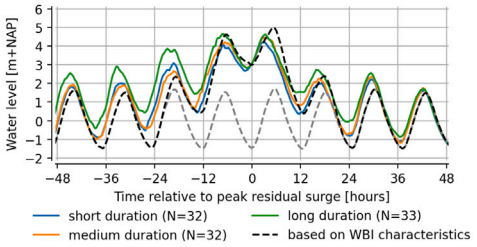

(d) Sea level hydrographs ($\varphi = 5.0$ h and direction West)

Fig. F.24. Normalized storm surge and sea level hydrographs for location Delfzijl, corresponding to a maximum surge height s of 4.5 meters, compared to the WBI schematization (black, dashed lines). The corresponding astronomical tide is depicted as a gray dashed line. The sea level hydrographs are presented for direction West and the three dominant tidal phases. The three colors represent the three duration classes (short, medium, long).

Data availability

Data will be made available on request.

References

van den Brink, H.W., 2020. Het gebruik van de ECMWF seizoensverwachtingen voor het berekenen van de klimatologie van extreme waterstanden langs de Nederlandse kust. Technical Report TR-385, KNMI, De Bilt.

Caspers, J., Kindermann, P., 2023. Hydraulic load model for the Dutch Shore - Analysis about the relevance of time aspects. Technical Report PR4529.20, HKV Lijn in Water, Lelystad.

Charnock, H., 1955. Wind stress on a water surface. Q. J. R. Meteorol. Soc. 81 (350), 639–640.

Chbab, H., 2015a. Basisstochasten WTI-2017. Statistiek en statistische onzekerheid. Technical Report 1209433-012-HYE-0007, Deltares, Delft.

Chbab, H., 2015b. Waterstandsverlopen kust. Wettelijk Toetsinstrumentarium WTI-2017. Technical Report 1220082-002-HYE-0003, Deltares.

Chbab, H., de Waal, H., 2017. Achtergrondrapport Hydraulische Belastingen Wettelijk Beoordelingsinstrumentarium 2017. Technical Report 1230087-008-HYE-0001, Deltares.

De Ronde, J., 1985. Wisselwerking tussen opzet en verticaal getij. Nota GWIO-85.003.. Technical Report, Rijkswaterstaat, dienst getijdewateren, Distrikt Zuidwest, Dordrecht.

de Valk, C., van den Brink, H., 2023. Update van de statistiek van extreme zeewaterstand en wind op basis van meetgegevens en modelsimulaties. Technical Report TR-406, KNMI.

de Valk, C., van den Brink, H., 2025. An appraisal of the value of simulated weather data for quantifying coastal flood hazard in the netherlands. Nat. Hazards Earth Syst. Sci. 25 (5), 1769–1788. http://dx.doi.org/10.5194/nhess-25-1769-2025.

Deltacommissie, 1961. Onderzoekingen betreffende de opzet van het Deltaplan en de gevolgen van de werken, Deel 5. Technical Report, Staatsdrukkerij- en uitgeverijbedrijf.

Diakomopoulos, F., Antonini, A., Bakker, A.M., Stancanelli, L.M., Hrachowitz, M., Ragno, E., 2024. Probabilistic characterizations of flood hazards in deltas: Application to hoek van holland (netherlands). Coast. Eng. 194, http://dx.doi.org/10.1016/J.COASTALENG.2024.104603.

Direktie Waterhuishouding en Waterbeweging, 1984. Waterstandfrekwenties op de Beneden Merwede en de Boven Merwede. Notanummer 61.002.17.. Technical Report, Distrikt Zuidwest, Dordrecht.

Dullaart, J.C., Muis, S., Moel, H.D., Ward, P.J., Eilander, D., Aerts, J.C., 2023. Enabling dynamic modelling of coastal flooding by defining storm tide hydrographs. Nat. Hazards Earth Syst. Sci. 23, 1847–1862. http://dx.doi.org/10.5194/nhess-23-1847-2023.

ECMWF, 2021. SEAS5 user guide. Technical Report, ECMWF, URL https://www.ecmwf.int/sites/default/files/medialibrary/2017-10/System5_guide.pdf.

Geerse, C., 2003. Probabilistisch model hydraulische randvoorwaarden Benedenrivierengebied.. Technical Report, HKV Lijn in Water en WL|Delft Hydraulics, Lelystad.

Geerse, C., 2020. Interaction between tide and surge. Technical Report PR4366.10, HKV Lijn in Water, Lelystad.

Geerse, C., Caspers, J., Kindermann, P., 2022. Hydraulic load model for the Dutch Shore - A statistical model for extreme hydraulic loads and corresponding time evolutions. Technical Report PR4529.20, HKV Lijn in Water, Lelystad.

Geerse, C., Rongen, G., Strijker, B., 2019. Schematization of storm surges. Technical Report PR3874.10, HKV Lijn in Water, Lelystad.

Gerritsen, H., de Vries, H., Philippart, M., 1995. The Dutch Continental Shelf Model. Coast. Estuar. Stud. 425–467. http://dx.doi.org/10.1029/CE047P0425.

Hersbach, H., Bell, B., Berrisford, P., Hirahara, S., Horányi, A., Muñoz-Sabater, J., Nicolas, J., Peubey, C., Radu, R., Schepers, D., Simmons, A., Soci, C., Abdalla, S., Abellan, X., Balsamo, G., Bechtold, P., Biavati, G., Bidlot, J., Bonavita, M., De Chiara, G., Dahlgren, P., Dee, D., Diamantakis, M., Dragani, R., Flemming, J., Forbes, R., Fuentes, M., Geer, A., Haimberger, L., Healy, S., Hogan, R., Hólm, E., Janisková, M., Keeley, S., Laloyaux, P., Lopez, P., Lupu, C., Radnoti, G., Rozum, I.P.d., Vamborg, F., Villaume, S., Thépaut, J., 2017. Complete ERA5 from 1940: Fifth generation of ECMWF atmospheric reanalyses of the global climate. Copernicus climate change service (C3S) data store (CDS).. http://dx.doi.org/10.24381/cds.143582cf, (Accessed on 04 Dec 2024).

Horseburgh, K., Wilson, C., 2007. Tide-surge interaction and its role in the distribution of surge residuals in the north sea.. J. Geophys. Res. 112 (C08003), http://dx.doi.org/10.1029/2006JC004033.

Janssen, H., 1990. Optimalisatie verdelingen voor max opzet als functie van de faseverdeling. SVKW-TOC-90.016.. Technical Report.

Jongejan, R., Kok, M., Nieuwjaar, M., Tánczos, I., 2016. Fundamentals of flood protection. Rijkswaterstaat, Expertise Netwerk Waterveiligheid.

Jonkman, S.N., Schweckendiek, T., 2015. Developments in levee reliability and flood risk analysis in the netherlands. Geotech. Saf. Risk V http://dx.doi.org/10.3233/978-1-61499-580-7-50.

MacPherson, L.R., Arns, A., Dangendorf, S., Vafeidis, A.T., Jensen, J., 2019. A stochastic extreme sea level model for the german baltic Sea Coast. J. Geophys. Res.: Ocean. 124, 2054–2071. http://dx.doi.org/10.1029/2018JC014718.

Muis, S., Aerts, J.C., Antolínez, J.A., Dullaart, J.C., Duong, T.M., Erikson, L., Haarsma, R.J., Apecechea, M.I., M., Bars, D.L., O'Neill, A., Ranasinghe, R., Roberts, M.J., Verlaan, M., Ward, P.J., Yan, K., 2023. Global projections of storm surges using high-resolution CMIP6 climate models. Earth' s Futur. 11, http://dx.doi.org/10.1029/2023EF003479.

National Center for Atmospheric Research Staff (Eds), 2022. The climate data guide: Climate forecast system reanalysis (CFSR). URL https://climatedataguide.ucar.edu/climate-data/climate-forecast-system-reanalysis-cfsr (Accessed on 04 Dec 2024).

Rijkswaterstaat, 2024. Rijkswaterstaat waterinfo. URL https://waterinfo.rws.nl (Accessed on 28 Oct 2024).

Tijssen, A., Diermanse, F., 2010. Storm surge duration and storm duration at Hoek van Holland. Technical Report, Deltares.

Van Dorland, R., Beersma, J., Bessembinder, J., Bloemendaal, N., Van Den Brink, H., Brotons Blanes, M., Drijfhout, S., Groenland, R., Haarsma, R., Homan, C., Keizer, I., Krikken, F., Le Bars, D., Lenderink, G., Van Meijgaard, E., Meirink, J.F., Overbeek, B., Reerink, T., Selten, F., Severijns, C., Siegmund, P., Sterl, A., De Valk, C., Van Velthoven, P., De Vries, H., Van Weele, M., Wichers Schreur, B., Van Der Wiel, K., 2023. KNMI National Climate Scenarios 2023 for the Netherlands. Technical Report, Royal Netherlands Meteorological Institute, De Bilt.

Verlaan, M., Zijderveld, A., De Vries, H., Kroos, J., 2005. Operational storm surge forecasting in the Netherlands: developments in the last decade. Philos. Trans. R. Soc. A: Math. Phys. Eng. Sci. 363 (1831), 1441–1453. http://dx.doi.org/10.1098/RSTA.2005.1578.

Zijderveld, A., Verboeket, R., Bosma, B.J., IJpelaar, R., 2022. Stormvloedrapport SR100. Stormvloeden tijdens stormen Eunice en Franklin van 18 t/m 21 februari 2022. Technical Report, Watermanagementcentrum Nederland, Lelystad.

Zijl, F., Zijlker, T., Laan, S., Groenenboom, J., 2022. 3D DCSM FM: a sixth-generation model for the NW European Shelf. Technical Report, Deltares.